

Zero bias conductance peak in Majorana wires made of semiconductor-superconductor hybrid structures

Chien-Hung Lin¹, Jay D. Sau², and S. Das Sarma¹

¹*Condensed Matter Theory Center and Joint Quantum Institute, Department of Physics, University of Maryland, College Park, Maryland 20742-4111, USA. and*

²*Department of Physics, Harvard University, Cambridge, MA 02138, USA.*

(Dated: October 31, 2018)

Motivated by a recent experimental report¹ claiming the likely observation of the Majorana mode in a semiconductor-superconductor hybrid structure²⁻⁵, we study theoretically the dependence of the zero bias conductance peak associated with the zero-energy Majorana mode in the topological superconducting phase as a function of temperature, tunnel barrier potential, and a magnetic field tilted from the direction of the wire for realistic wires of finite lengths. We find that higher temperatures and tunnel barriers as well as a large magnetic field in the direction transverse to the wire length could very strongly suppress the zero-bias conductance peak as observed in Ref.[1]. We also show that a strong magnetic field along the wire could eventually lead to the splitting of the zero bias peak into a doublet with the doublet energy splitting oscillating as a function of increasing magnetic field. Our results based on the standard theory of topological superconductivity in a semiconductor hybrid structure in the presence of proximity-induced superconductivity, spin-orbit coupling, and Zeeman splitting show that the recently reported experimental data are generally consistent with the existing theory that led to the predictions for the existence of the Majorana modes in the semiconductor hybrid structures in spite of some apparent anomalies in the experimental observations at first sight. We also make several concrete new predictions for future observations regarding Majorana splitting in finite wires used in the experiments.

I. BACKGROUND

The search for solid state Majorana modes, which are localized quasiparticles with non-Abelian braiding statistics and a direct realization of the Majorana operator, has created a great deal of recent interest in the whole physics community⁶, partly because of the great mystique associated with Majorana and partly because of the prospects for topological quantum computation using solid state Majorana quasiparticles. The most experimentally promising among the many theoretical proposals for solid state Majorana fermions is the semiconductor-superconductor hybrid structures²⁻⁵ where the ordinary s-wave superconducting proximity effect induced in the semiconductor is modified by the intrinsic spin-orbit coupling in the semiconductor and an externally applied Zeeman spin splitting. The solution of the resultant superconducting gap equations, often called the Bogulibov-De Gennes (BdG) equations, in the presence of both spin-orbit coupling and spin splitting explicitly shows a quantum phase transition in the nature of the superconducting phase as a function of the Zeeman splitting (which can be controlled by an external magnetic field). The lower magnetic field part of the superconducting phase is an ordinary non-topological s-wave superconductor with a suppressed gap due to the finite spin splitting which eventually gives way to a topological (effectively a p-wave) superconducting phase at large spin splitting when the original proximity-induced s-wave gap is completely suppressed. The Majorana mode appears naturally as a stable zero-energy solution inside the gap of this topological superconducting phase. It has

been shown that the existence of the Majorana quasiparticle would give rise to a conductance peak at zero energy inside the nominal p-wave superconducting gap of the topological phase. The experimental observation of this predicted zero energy conductance peak inside the superconducting gap at finite magnetic field in the semiconductor-superconductor hybrid structure is therefore believed to be the necessary evidence in support of the solid state Majorana mode¹.

It is useful to compare our semiconductor nanowire model for the Majorana modes with the original 1D Majorana wire model introduced by Kitaev ("the Kitaev model"). In the Kitaev model, the topological p-wave superconductivity is assumed explicitly by making the system a spinless p-wave superconductor. In fact, Kitaev in his paper⁸ goes on to discuss at quite some length the possibility of realizing such a topological 1D spinless p-wave superconductivity in nature, concluding that the most suitable systems for realizing such spinless 1D p-wave superconductivity are quasi-1D organic superconductors involving charge and spin density wave ground states, which were already proposed as possible Majorana-carrying systems by Sengupta et al.⁹ who in fact also pointed out that the zero bias conductance peak associated with such Majorana modes would be quantized. It is a curious historical coincidence that Kitaev in his original paper explicitly rejected both spin-orbit coupling and Zeeman splitting as possible physical mechanisms for producing 1D spinless p-wave superconductivity! The current activity in 1D semiconductor Majorana wires started from the work of Sau et al.² who showed that in 2D semiconductors with proximity s-wave superconductivity induced by a nearby ordinary s-wave

superconducting metal, the topological superconductivity ("2D chiral p-wave superconductor") would naturally arise in the presence of spin splitting and spin-orbit coupling provided that the spin-splitting is large enough to overcome the trivial s-wave superconductivity. It was soon realized³⁻⁵ that this 2D chiral topological superconductivity can easily be modified to 1D helical topological superconductivity by considering 1D semiconductor nanowires rather than 2D semiconductor heterostructures with the spin splitting being introduced by an external magnetic field. This helical 1D p-wave superconductor is an effective realization of the 1D Kitaev model, but it is not identical to the Kitaev model. For example, the topological superconductivity in the 1D nanowires exists only above a finite value of the spin splitting with only trivial non-topological superconductivity existing at weaker magnetic field values. Also, the superconducting gap depends explicitly on the spin splitting and the spin-orbit coupling in the semiconductor nanowires instead of being just effective theoretical parameters.

II. INTRODUCTION

In a recent presentation¹, the likely experimental observation of the theoretically-predicted²⁻⁵ zero-energy Majorana modes in semiconductor nanowires, in close proximity to an ordinary (i.e. s-wave) superconductor and in the presence of an external magnetic field applied along the wire, has been reported. This experimental observation of the predicted zero bias peak and the associated implication that this may finally be the real-life evidence for the existence of the elusive (and so-far purely theoretical) Majorana mode have created tremendous excitement⁶ in the general scientific community. Given the great significance of the possible experimental discovery of the Majorana mode, it is therefore of utmost importance to ensure that all aspects of the experimental discovery in Ref.[1] are indeed consistent with the theoretical expectations and there are no loose ends. This is particularly true in view of the facts that the experimental observation precisely follows theoretical predictions for the existence of the Majorana zero energy mode in semiconductor-superconductor hybrid structures and that zero bias peaks could arise in superconductors and semiconductors from a variety of physical effects such as Andreev or Shiba bound states, Kondo resonances, etc. Our work presented in this paper aims at a qualitative understanding of several interesting features of the experimental observation to ensure that the observation is consistent with the expectations of the BdG theory for the Majorana mode in semiconductor-superconductor structures.

In the current work, we theoretically investigate some of the peculiar aspects of the experimental observations in Ref.[1] which were not directly or explicitly predicted earlier^{2-5,7-11} in the extensive theoretical work

leading to the experimental observation of the Majorana mode although some of the aspects we discuss in our work were implicit in the theory. The experimental observation specifically concentrates on the study of a zero-bias-conductance peak (ZBCP) in the current (I)-voltage(V) differential conductance ($\frac{dI}{dV}$) of the tunneling spectroscopy of an InSb nanowire on superconducting NbTiN, which manifests itself only in the presence of an external magnetic field B_x ($\gtrsim 0.1$ T) oriented along the wire (taken to be the x -axis in this paper). The existence of this ZBCP in Ref.[1] for $B_x \neq 0$ has been claimed to be the verification of the theoretical prediction for the existence of the zero-energy Majorana mode²⁻⁵ in the wire. The zero-energy Majorana mode exists as localized quasiparticles at the ends of the superconducting wire and is a manifestation of the system being in a chiral p -wave topological superconducting (TS) phase as envisioned more than a decade ago^{8,9}. The theory predicts^{2-5,7,10} the presence of the TS phase for $V_x > V_c = \sqrt{\Delta^2 + \mu^2}$, i.e. $B_x > B_c = V_c/g\mu_B$ with $V_x = g\mu_B B_x$ being the Zeeman field in the wire associated with B_x , and Δ, μ are the superconducting gap and the chemical potential respectively in the wire. For $B_x < B_c$ (or $V_x < V_c$) the system is in an ordinary non-topological (i.e. s-wave) superconducting phase (NTS) which in the presence of the finite Zeeman splitting V_x makes a topological quantum phase transition^{2-5,7-12} to the TS phase for $V_x > V_c$ (i.e. $B_x > B_c$). The TS phase has the Majorana modes localized at the ends of the wire and the associated ZBCP at zero energy in the middle of the superconducting gap. The NTS phase on the other hand has no structure, except perhaps some Andreev bound states (ABS) at generic non-zero energies, within the superconducting gap. The existence of a robust ZBCP in the differential tunneling conductance has therefore been predicted^{2-5,7,9-11,13} to be the necessary condition for the observation of the Majorana mode, and its observation in Ref.[1] is an important experimental milestone providing perhaps the first definitive signature for the Majorana fermion in a solid state system.

Given the key importance of the subject matter, namely, the possible experimental discovery of the emergent Majorana mode in the topological superconductor system, it is somewhat disconcerting that some of the observed experimental features are unexpected and somewhat inconsistent with the existing theoretical predictions in the literature although most of the findings in Ref.[1] are, in fact, completely consistent with the theoretical predictions (e.g. the existence of ZBCP only above a critical value of B_x). We concentrate in the current work on three features of the experiment which, in our opinion, require special attention: (1) the observed ZBCP is much (by more than an order of magnitude) weaker than the predicted^{9,11,13-15} canonical quantized value of $2e^2/h$ expected for the Majorana zero energy mode; (2) a peculiar and unexpected splitting of the ZBCP at high values of V_x (for $B_x \gtrsim 0.5$ T) observed in Ref.[1]; (3) the predicted behavior of the ZBCP in

the presence of an additional transverse component V_y of the Zeeman field associated with an applied magnetic field component $B_y (= V_y/g\mu_B)$ along the direction of the spin-orbit coupling field (y -axis) which is known¹⁶ to be transverse to the length to the wire. Of the three issues theoretically considered in this work, the first two are directly motivated by the experimental data presented in Ref.[1] where a strongly suppressed ZBCP (with a differential conductance value substantially below $2e^2/h$) and a splitting of the ZBCP into a doublet at high values of B_x are both observed. Item (3) in our work is alluded to in Ref.[1], and our work here provides the numerical results for the expected experimental observation when the applied in-plane \vec{B} field is tilted at an angle θ to the wire length direction, i.e. $(B_x, B_y) = (B \cos \theta, B \sin \theta)$, which gives $(V_x, V_y) = (g\mu_B B \cos \theta, g\mu_B B \sin \theta)$ where g, μ_B are the Lande g -factor and the Bohr magneton respectively.

The most important new qualitative feature of our theoretical work presented in this work is considering realistic experimental systems, in particular, finite wire lengths and finite temperatures as well as finite tunneling barrier heights. We find that the finiteness of the nanowires is a fundamental constraint in the ideal realization of the Majorana zero energy mode, and most of our interesting and important results arise directly from our keeping wire lengths finite as in the experimental systems. The reason for the qualitative importance of the finite wire length is rather obvious. The external magnetic field suppresses the superconducting gap, both in the NTS and the TS phase, thus enhancing the coherence length which varies inversely as the gap energy. When the enhanced coherence length becomes comparable to the wire length, the two end Majorana modes start 'seeing' each other, leading to an energy splitting. This effect turns out to be of qualitative importance, affecting for example the conductance quantization of the Majorana ZBCP even at $T = 0$ in contrast to the ideal infinite wire case where the ZBCP is always quantized at $2e^2/h$ in the $T = 0$ limit.

The quantization of the ZBCP predicted for Majorana fermions^{9,11,13,15} is a result that is valid only in the zero-temperature limit. In contrast, the high-temperature limit has a more conventional resonant scattering Fano-form^{3,15,17} with a height proportional to $\Gamma/k_B T$ and a width proportional to the thermal energy $k_B T$, for $k_B T \gg \Gamma$ with Γ/\hbar being the tunneling rate between the Majorana bound state and the lead. The tunneling rate Γ/\hbar depends on the transparency of the tunneling barrier, and is not easily experimentally controllable—in fact, the barrier transparency and hence the tunneling rate is simply unknown in the experimental situation. In the part of this work which focuses on Item (1), we show how the tunneling conductance crosses over from the low-temperature to the high-temperature limit and establish that for reasonable parameters, it is indeed possible to have a dramatic suppression of the ZBCP as seen in Ref.[1]. In addition, from our numerical calculations for the realistic parameters, we have found that even at $T = 0$, the ZBCP can be suppressed below its quan-

tized value for sufficiently small tunneling rate Γ because of finite size effects. In particular, such a $T = 0$ suppression of ZBCP happens when Γ becomes comparable to the splitting between the end Majorana fermions, which may be the case for the few micron long wires in Ref.[1] together with the tunneling rates Γ inferred from the measured conductance. The splitting between end Majoranas is invariably present in real wires where the two end Majoranas have some finite overlap, leading to a lifting of their precise zero energy status. The splitting of the ZBCP as a function of V_x , which is discussed as part of Item (2) in this paper is a finite size effect, which is likely to be relevant for the experiments in Ref.[1], but as far as we are aware has not been discussed in the literature except in the idealized situation¹⁸. The predictions in the literature, which are restricted to infinite wires, show that the Majorana fermion must be robust for large Zeeman fields in the case of narrow wires where the inter-sub band spacing is much larger than the Zeeman splitting. The numerical results presented in this paper show that for finite wires, even in the narrow wire limit, the ZBCP is split for large V_x . The splitting of the ZBCP arises from overlap of the Majorana fermion wave-functions as has been previously discussed in the context of p -wave superconductors¹⁸. To the best of our knowledge, our work is the only existing result in the literature for the Majorana splitting in finite wires in the presence of spin-orbit coupling and Zeeman splitting. Finally in the context of Item (3), we discuss the effect of the angle of the Zeeman potential on the ZBCP. Consistent with previous theoretical work³, which shows that the proximity-induced quasiparticle gap vanishes in the wire for $V_y > \Delta$, we find that the ZBCP vanishes above a threshold value of V_y .

We emphasize that our goal in this work is not to develop a new theory for the Majorana modes in the semiconductor nanowires, but to extend and generalize the existing theory²⁻⁴ leading to the prediction of the Majorana mode in semiconductor hybrid structures, to finite wire lengths, temperatures, and barrier heights as well as to large Zeeman splitting (along arbitrary directions also) to see whether the features arising out of the standard theory are consistent with the observations of Ref.[1]. Of course, theory by itself cannot answer the question whether the observations in Ref.[1] are really the isolated Majorana modes predicted by theory²⁻⁴ or are some disorder or multi-mode wire effect. Instead our goal is to show that some of the qualitative features of the experiment, which are not immediately consistent with the results explicitly predicted in previous works²⁻⁴, are indeed consistent with the experiment. therefore, it is important to discern which features of the experimental data are in direct agreement with the theory extended to include finite wire length, finite temperature, finite barrier height, and large Zeeman field. Such a comparison, as carried out in this work, between the extended standard theory and the data of Ref.[1] will help indicate whether the experiment¹ really is consistent with a Majorana in-

terpretation and also whether new ideas are essential to understand some features of the data. As discussed in more detail in Sec. VI, we intentionally avoid discussing issues such as disorder and the multi-band effects, since these effects would complicate the conclusions by introducing more unknowns into the theory. Moreover, as elaborated further in Sec. VI, the experimental data in Ref.[1] appears to use wires with relatively long mean-free paths (300 nm) and have large sub-band spacings so that such effects are unlikely to change our conclusions in a qualitative way. In this context, it is also important to emphasize that the finite wire length automatically implies a crossover in the behavior of the Majorana mode when the magnetic field induced suppression of the superconducting induced gap leads to the coherence length becoming comparable to or larger than the wire length. This physics is qualitatively new in our work (although it is implicit in the earlier works) because a finite wire length allows the two Majorana modes to overlap with each other leading to a splitting which is by definition impossible in an infinite wire at any magnetic field. Since the experiments are always done in finite wires, our work provides a crucial extension of the standard theory in order to understand or interpret the experimental results even at a qualitative level.

III. THEORY

The physical system²⁻⁴ for studying Majorana fermions includes a strongly spin-orbit coupled semiconductor (SM), proximity-coupled to an *s*-wave superconductor (SC) and imposed to a Zeeman field. Without loss of generality, we consider a finite 1D SM nanowire along the \hat{x} direction, the spin-orbit interaction α_R , being along the y axis, and a Zeeman field $\vec{V} = (V_x, V_y)$. Also the wire is in contact with a superconductor, with proximity induced pairing strength Δ . The continuous BdG Hamiltonian for the system is

$$H = \left(-\frac{\hbar^2}{2m} \partial_x^2 - \mu \right) \tau_z + V_x \sigma_x + V_y \sigma_y + i\alpha_R \partial_x \sigma_y \tau_z + \Delta \tau_x. \quad (1)$$

μ is the chemical potential. The Pauli matrices σ, τ operate in spin and particle-hole space, respectively. For numerical convenience, it is standard to study the BdG equation in a discrete lattice tight-binding approximation with no loss of generality and with fewer unknown parameters. Under the lattice approximation, we can

map (1) to a tight-binding model

$$H = \sum_{i,j,\sigma} t_{ij} c_{i\sigma}^\dagger c_{j\sigma} - \sum_{i,\sigma} \mu_i c_{i\sigma}^\dagger c_{i\sigma} \quad (2)$$

$$+ \sum_{i,\sigma\sigma'} \frac{\alpha_i}{2} \left[c_{i+1\sigma}^\dagger (i\sigma_y)_{\sigma\sigma'} c_{i\sigma'} + H.c. \right]$$

$$+ \sum_{i,\sigma} c_{i\sigma}^\dagger (V_x(i) \sigma_x + V_y(i) \sigma_y)_{\sigma\sigma'} c_{i\sigma'}$$

$$+ \sum_i \Delta_i \left(c_{i\uparrow}^\dagger c_{i\downarrow}^\dagger + H.c. \right) \tau_x$$

The first contribution describes hopping or the kinetic energy along the length (i.e. the x -axis) of the wire, the second term represents the Rashba spin-orbit interaction, the third term is the Zeeman field and the last term shows the proximity-induced pairing term. $c_{i\sigma}^\dagger, c_{i\sigma}$ denote electron creation and annihilation operators, respectively. We include only nearest-neighbor hopping with $t_{ij} = -t_0$ and also include an on-site contribute $t_{ii} = 2t_0$ that shifts the bottom of the energy spectrum to zero energy. The chemical potential μ is calculated from the bottom of the band. In the long wavelength limit, the tight binding model reduces to the continuum Hamiltonian (1) with $t_0 = \hbar^2/2m^*a^2$ and Rashba spin-orbit coupling $\alpha_R = \alpha a$ with lattice constant a . In the numerical calculations we use a set of parameters consistent with the properties of InSb, as in Ref.[1], and choose the effective mass $m^* = 0.015m_e$, spin-orbit coupling $\alpha_R = 0.2 \text{ meV \AA}$, and $g\mu_{B, InSb} = 1.5 \text{ meV/T}$. We also use $\Delta = 0.5 \text{ meV}$ and the length of the wire to be $4.5 \mu\text{m}$. These parameters are roughly consistent with the experimental conditions of Ref.[1] although we are not interested in fine-tuning parameters for quantitative agreement with the data because there are far too many unknown parameters in the experiment. We choose the tight binding numerical lattice parameter $a = 15 \text{ nm}$, which is chosen so that the band-width $2t_0 \gg V, \Delta, \mu$ and thus the tight binding approximation itself would not introduce any artifacts into our results. The length of the wire $L = 4.5 \mu\text{m}$ then corresponds to $N = 300$ sites. We mention here that the SC proximity effect has now been observed by several groups in the SC/SM hybrid systems including both InSb nanowires^{1,19,20} and InAs nanowires^{21,22}. Thus, the effective model given by Eq.2, which is the starting point for our theory, is an appropriate model for the SM nanowire in the presence of spin-orbit coupling, Zeeman splitting, and proximity-induced superconductivity.

To calculate the differential conductance measured from tunneling into the end of the superconducting nanowire, we have to study the current flowing into the wire contacted through a barrier region at one end with a lead by using the Blonder-Tinkham-Klawijk (BTK) formalism.²³ The main idea is to get the reflection and transmission coefficients by solving a BdG eigen-equation with some initial conditions. The current and conductance can be expressed in terms of these coefficients. Given that the experiment involves many unknown pa-

rameters controlling many interfaces (e.g. SC/SM, tunneling barrier/SM, various gates to control the barriers and chemical potential), our goal is to utilize the simplest possible model with the fewest number of parameters which would be capable of capturing the underlying qualitative physics of the experiment in finite wires. The BdG-BTK formalism provides the simplest qualitative basis for the theoretical modelling of the experimental system in Ref.[1].

More precisely, we start with the tight-binding Hamiltonian (2) with open boundary conditions so that the part $i = 0, 1, \dots, m_L$ are in the lead with no superconductivity and the sites $i = m_L + 1, \dots, N$ are in the superconducting nanowire. The barrier region is modeled as a variation in the local chemical potential $\mu_i \rightarrow \mu_i - U$ for the sites $i = m_L - 2, \dots, m_L + 2$, where U is the tunnel barrier height. To calculate the reflection and transmission coefficients at energy E , we note that since the lead is normal (without spin-orbit coupling), the incoming mode can be taken to be purely electron-like. The reflected amplitudes can be normal $r_{N,\sigma,\sigma'}$ or anomalous $r_{A,\sigma,\sigma'}$. Here σ is the spin of incoming electron and σ' is the spin of the reflected electron and hole. The BdG equations that determine the reflected coefficients are

$$\sum_{n=0,N} (H_{m,n} - E\delta_{m,n}) \Psi_n = 0 \text{ for } m = 1, \dots, N$$

$$\Psi_{n=0} = \begin{pmatrix} \delta_{\sigma,\uparrow} \\ \delta_{\sigma,\downarrow} \\ 0 \\ 0 \end{pmatrix} + \begin{pmatrix} r_{N,\sigma,\uparrow} \\ r_{N,\sigma,\downarrow} \\ r_{A,\sigma,\uparrow} \\ r_{A,\sigma,\downarrow} \end{pmatrix}$$

$$\Psi_{n=1} = \begin{pmatrix} \delta_{\sigma,\uparrow} \\ \delta_{\sigma,\downarrow} \\ 0 \\ 0 \end{pmatrix} e^{ik_e a} + \begin{pmatrix} r_{N,\sigma,\uparrow} \\ r_{N,\sigma,\downarrow} \\ 0 \\ 0 \end{pmatrix} e^{-ik_e a}$$

$$+ \begin{pmatrix} 0 \\ 0 \\ r_{A,\sigma,\uparrow} \\ r_{A,\sigma,\downarrow} \end{pmatrix} e^{ik_h a}.$$

The first equation is the BdG equation in the superconducting wire, while the latter two equations express the wave-functions in the lead in terms of the reflection coefficients. These equations need to be solved for both $\sigma = \uparrow, \downarrow$. In the above k_e is the wave-vector in the lead at energy E so that

$$\frac{k_e^2}{2m} - \mu_{lead,\sigma} = E$$

where μ_{Lead} is the chemical potential of the lead, while k_h satisfies

$$\frac{k_h^2}{2m} - \mu_{lead,\sigma} = -E.$$

The voltage-bias V of the lead determines the occupancy of the incident electrons. Electrons are incident on the superconductor from energy $E = -\mu_{lead}$ to $E = V$. The

states with normal reflection do not contribute to the current. Thus, the current will be

$$I = \sum_{\sigma} \int_{-\mu_{lead,\sigma}}^V dE \sum_{\sigma'} |r_{A,\sigma,\sigma'}(E)|^2$$

which implies a conductance (in unit of $2e^2/h$)

$$\frac{dI}{dV} = \sum_{\sigma,\sigma'} |r_{A\sigma\sigma'}(E = V)|^2.$$

Technically for negative bias voltages $V < 0$, one needs to consider holes below the fermi-energy incident from the right with energy $E = -V > 0$ and then Andreev reflected at the interface and becoming electrons. However, such processes are related by particle-hole symmetry to Andreev reflection of negative energy electrons. Therefore, one does not need to calculate the Andreev reflection process separately since it is automatically incorporated in our BdG-BTK formalism.

To generalize to finite temperatures all one needs to do is to broaden the conductance with the derivative of the Fermi-function in the usual manner

$$G(V, T) = \int d\varepsilon G_0(\varepsilon) \frac{1}{4T \cosh^2((V - \varepsilon)/2T)}$$

with $G_0(\varepsilon)$ the zero temperature conductance at energy ε .

We present our numerical results for the calculated tunneling conductance as a function of bias voltage and other relevant experimental tuning parameters in Figs.1-5 to be compared with the experimental data of Ref.[1]. We first mention the fact that the (Majorana) properties of the real experimental system depend on (at least) ten independent parameters (many of which are unknown). These parameters include temperature, tunneling barrier (which in all likelihood depends on several unknown parameters determined by the details of the interface and the control gates), Zeeman fields (V_x and V_y), spin-orbit coupling, chemical potential, the induced superconducting gap (which in turn depends on several parameters such as the semiconductor-superconductor hopping amplitude, disorder, and the parent gap in NbTiN), the parameters defining the 1D confinement in the wire (which requires at least four independent parameters for confinement along y and z directions), wire length (L) along the wire, and disorder (which by itself would necessitate several independent parameters for its description since in principle there could be long-ranged and short-ranged random impurities in the wire as well as interfacial roughness at the semiconductor-superconductor interface). No meaningful theory, beyond mere data fitting, can of course attempt to include all these parameters. In the current work we are interested in the fundamental question of whether a minimal theoretical model can capture the basic qualitative findings of Ref.[1], and as such we ignore all the complications, concentrating on the single subband 1D model in the absence of disorder

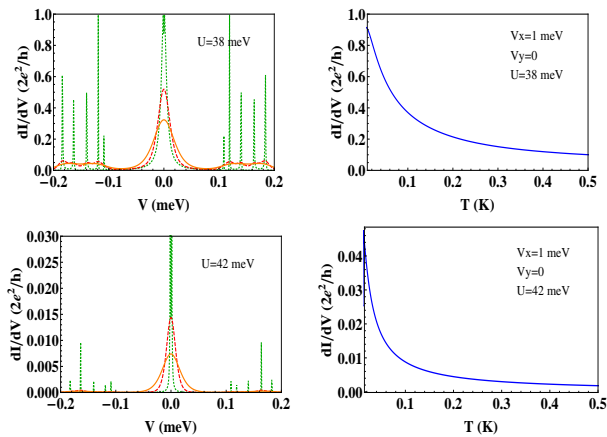


FIG. 1: (Two Left Panels) The differential conductance for a fixed Zeeman potential $\mathbf{V} = (1, 0)$ meV and different tunneling barrier $U = 38$ and 42 meV. The green dotted, red dashed and orange lines denote different temperature $0, 60, 120$ mK, respectively. (Two Right Panels) Zero bias conductance peak as a function of temperature for Zeeman potential $\mathbf{V} = (1, 0)$ meV and different tunneling barrier $U = 38$ and 42 meV, respectively. The peak decreases monotonously with temperature. ($L = 4.5\mu\text{m}$, spin-orbit coupling $\alpha = 0.2$ meV \AA , induced pairing potential $\Delta = 0.5$ meV)

within a tight-binding BdG-BTK formalism. Our work should be construed as a zeroth order effective model of the experiment which should be the starting point for future quantitative and realistic theoretical studies when the details of the experimental parameters become available.

IV. RESULTS

In Fig.1 we show our calculated differential conductance dI/dV as a function of the tunneling bias voltage V (which should not be confused with the Zeeman fields V_x, V_y) for two different tunnel barriers and three different temperatures for $V_x = 1$ meV and $V_y = 0$. (This choice of $\mathbf{V} = (V_x, V_y)$ guarantees that the system is in the TS phase satisfying $V_x > \sqrt{\Delta^2 + \mu^2}$ for our choice of system parameters corresponding to Ref.[1].) In the third panel of Fig.1, we depict $\frac{dI}{dV}$ of the ZBCP itself as a function of T for two values of U . These results manifestly establish that the canonical quantized value of $2e^2/h$ is clearly an unphysical theoretical limit achievable only as $T \rightarrow 0$ (and for low values of U). For reasonable values of U and T , our calculated value of ZBCP in Fig.1 could easily be one to two orders of magnitude smaller than $2e^2/h$, thus providing a satisfactory probable explanation for the weak strength of the ZBCP observed in Ref.[1]. We note that in our model, low values of U correspond to the more transparent barrier with higher conductance values—our numerical results clearly indicate that the ideal Majorana

conductance of $2e^2/h$ is unphysical even in the extreme low-temperature limit since the tunnel barrier U is never likely to be very small (or equivalently the transparency to the Majorana is not likely to be large). Our work leads immediately to the somewhat disappointing conclusion that the full Majorana spectral strength may never be achievable in the standard experimental set ups for measuring dI/dV since it would be very hard to get to the ideal limit of both T, U being very small (compared with the induced topological gap). Without our numerical results, this would not be apparent. Since the conductance calculated for the larger barrier height in Fig. 1 is found to be significantly below the quantized conductance even at $T = 0$, it is clear that the suppression of conductance in Fig. 1 is not purely the previously studied finite temperature effect^{11,17}. Of course, as mentioned in the Introduction, this finding of ours, namely that the Majorana tunneling differential conductance is not quantized even at $T = 0$ for finite U is valid only for finite wires since it is well-established that in the thermodynamic limit at $T = 0$ the Majorana conductance is necessarily quantized to a value of $2e^2/h$. The key here is that in finite wires the two end Majoranas always overlap, and one must have the tunneling barrier low enough for this overlap to be unimportant in determining the conductance quantization—thus for very long wires the conductance quantization will be valid up to very large values of U , but for short wires, the value of U must be quite low. Our finding of the strong suppression of the ZBCP in short wires even in the $T = 0$ limit due to the tunnel barrier effect (coupled with the Majorana overlap) is a new and somewhat unexpected result, which is consistent with the experimental finding of a saturation of the ZBCP at low temperatures¹. While splitting of the MFs resulting from the finite length of the wire is expected to suppress the ZBCP because splitting of the MFs removes the zero-energy state responsible for the ZBCP, one would expect such splitting to result in a split ZBCP rather than one that is simply reduced in magnitude. A split ZBCP should be discernible in experiments at low temperatures and in this case the splitting of the MFs would be easy to determine from the experimental results. Similarly, a reduction of the ZBCP from finite temperature would lead to a temperature dependent ZBCP, whose width is comparable to $k_B T$. Our results plotted in Fig. 1 show that for an intermediate regime of the barrier height, U , the finite overlap of the MFs can suppress the ZBCP without leading to an observable splitting of the ZBCP. Extremely large barrier heights U lead to peak width, which is dominated by temperature, and a temperature-dependent ZBCP height. Very low temperatures T and high barrier heights could in principle lead to a regime where a split conductance is observed. On the other hand, low temperatures and a barrier with a transparency smaller than the finite size splitting would result in a ZBCP, which is at the same time independent of temperature and also have a ZBCP height that is significantly smaller than $2e^2/h$. Our results show that

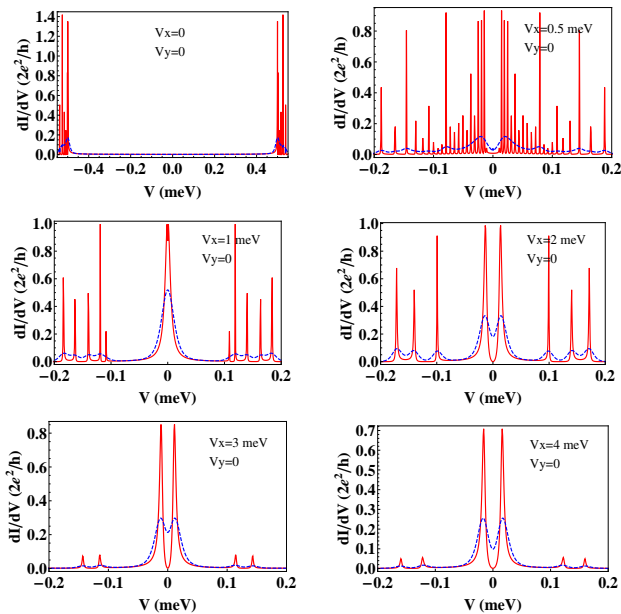


FIG. 2: The differential conductance for a fixed $V_y = 0$ meV and different $V_x = 0, 0.5, 1, 2, 3, 4$ meV. The red solid and blue dashed lines denote temperatures $T = 0$ and 60 mK, respectively. At $V_x = 1$ meV, the system is in the topological phase with quantized ZBCP. For length $L = 4.5 \mu\text{m}$, the Zeeman splitting $V_x \gg 1$ meV reduces the gap, and leads to a stronger overlap between the MFs that results in a splitting of the ZBCP peaks. Additionally the finite temperature will decrease ZBCP. (Parameters used in the plot: $U = 38$ meV, $L = 4.5 \mu\text{m}$, spin-orbit coupling $\alpha = 0.2$ meVÅ, induced pairing potential $\Delta = 0.5$ meV)

finite size effects can suppress a ZBCP significantly below $2e^2/h$, without the peak being temperature-independent or split.

In Fig.2, we show our calculated magnetic field or Zeeman splitting V_x dependence ($V_y = 0$) of dI/dV for two fixed temperatures keeping all other parameters fixed. The interesting result here in partial agreement with Ref.[1] is the splitting of the ZBCP for large ($V_x \geq 2$ meV) values of the Zeeman splitting. This ZBCP splitting arises from the wire length ($L = 4.5 \mu\text{m}$) being finite (both in our simulations and in Ref.[1]), which leads to the possibility of the two Majorana modes localized at the two ends of the wire to hybridize^{18,24} causing the splitting of the ZBCP. (The double-peak structure of the ZBCP is apparent in Ref.[1] for the applied magnetic field above ~ 0.48 T where two peaks around zero bias can be seen in the data.) The Majorana hybridization effect (and consequently the splitting of the ZBCP) is exponentially suppressed for smaller values of $V_x (> V_c)$ still within the TS phase since the superconducting gap is large. With increasing V_x , the gap is eventually suppressed as V_x^{-1} , which increases the coherence length, leading to an effective overlap between the Majorana modes localized at the two ends of the wire. There is

nothing mysterious about the splitting of the ZBCP at high values of V_x where the induced gap is small in the TS phase; this is expected– the important point is our finding that this happens in the same range of V_x values in our theoretical modeling as it does in the experiment. Interestingly for the parameters of the problem in Fig.2, we find the Zeeman induced splitting of the ZBCP to be only weakly dependent on Zeeman field. In particular, consistent with the data in Ref.[1] our calculated ZBCP splitting (~ 0.02 meV) in Fig.2 is much smaller than the applied Zeeman field ($V_x \sim 2 - 4$ meV) causing this splitting– this implies that the ZBCP splitting is not a trivial spin splitting either in our theory or in the experiment. As already mentioned above, the ZBCP splitting in the theory has its origin in the splitting of the Majorana zero energy mode due to the finite overlap of the two end Majorana localized wavefunctions overlapping due to the finite length and the high field situation, as predicted originally in Ref.[18]. We emphasize that the ZBCP splitting depends on increasing V_x in a nontrivial manner and is not simply a Zeeman splitting going as linear in B, which serves to distinguish the high-field Majorana splitting from any run-of-the-mill Zeeman splitting arising in the experimental situation.

The results presented in Fig.2 clearly indicate that the ZBCP splitting (i.e. the Majorana splitting in finite wires) as a function of the Zeeman field V_x , as was first predicted theoretically in Refs.[18] and [24] in a slightly different context. In fact, the splitting oscillates with the magnetic field V_x since it is an oscillatory function of the superconducting coherence length^{18,24}. This feature was also observed in the numerical work of Ref.[14]. We discuss this Majorana splitting in more details in discussing Fig.6 below, but the oscillatory behavior is already apparent in the results for the various V_x values shown in Fig.2 for smaller values of V_x .

The observed high-field (≥ 0.48 T) splitting of the ZBCP in Ref.[1] could thus probably arise from a finite wire length effect in the high field regime. Of course a quantitative comparison with experiment of the exact nature of the splitting of the ZBCP would require a systematic determination of the disorder and field configuration of the experiment. Also, the experimental data in Ref.[1] unfortunately end around 0.5 T value of the magnetic field, and it is therefore not possible right now to quantitatively compare the field dependence of our numerical finding of the ZBCP splitting arising from the Majorana overlap with the experimental observation. Hopefully, our theory will motivate further high-field studies so that the dependence of the ZBCP splitting on V_x can be compared between experiment and theory.

It is known^{18,24} that the Majorana splitting due to the overlap of two Majorana modes decays exponentially with their separation with the characteristic decay length being the superconducting coherence length. The main physics of the enhanced splitting with increasing V_x found in Fig.2 is thus the physics of the enhancement of

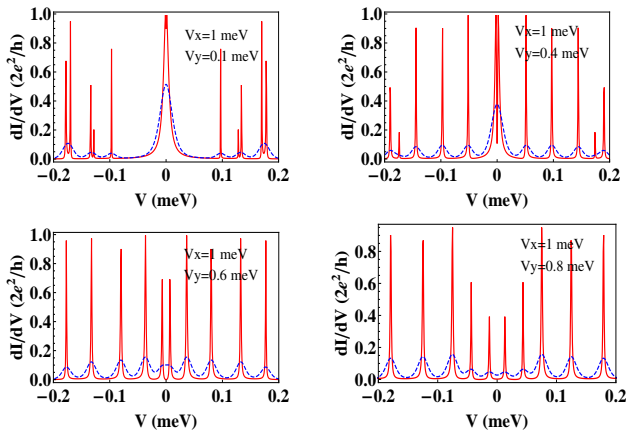


FIG. 3: The differential conductance for a fixed $V_x = 1$ meV and different $V_y = 0.1, 0.4, 0.6$ and 0.8 meV. The red solid and blue dashed denote temperatures $T = 0$ and 60 mK, respectively. At $V_x = 1$ meV, the system is in the topological phase with quantized ZBCP. V_y will reduce the quasi-particle gap and hence suppress the ZBCP. Finite temperature also reduces the ZBCP. ($U = 38$ meV, $L = 4.5 \mu m$, spin-orbit coupling $\alpha = 0.2$ meVÅ, induced pairing potential $\Delta = 0.5$ meV)

the coherence length due to the gap suppression by the external magnetic field. Such a splitting with increasing V_x is thus expected at high field values, but the important thing to note is that the splitting is consistent with the experimentally observed ZBCP splitting in the data of Ref.[1], lending credence to the claim that Ref.[1] is really exploring Majorana physics. Note that in an infinite system, such a splitting would never arise and the ZBCP will never split no matter how large V_x is. It is also known that in addition to the decay of the MF splitting in finite systems, characterized by the separation between the MFs normalized to the superconducting coherence length, the splitting also shows a characteristic oscillatory behavior as a function of the coherence length itself. In Fig.2, V_x is kept fixed in each panel, so these oscillations are not apparent, but we discuss these MF splitting oscillations as a function of V_x (through the enhancement of the coherence length by V_x) in the Sec. V of the paper (see, e.g., Fig.6(d) which explicitly shows the oscillation as a function of V_x).

Having provided reasonably realistic probable explanations for the two observed puzzling features of Ref.[1], namely, the suppressed values of ZBCP (Fig.1) and the splitting of ZBCP (Fig.2), we now consider the effect of a Zeeman field V_y in the spin-orbit coupling direction (i.e. transverse to the wire length). If $V_y \gg V_x$, we expect the ZBCP to disappear even if the system remains in the TS phase in accordance with the invariant Pfaffian calculation²⁵. This is because a large $V_y > \Delta$ is known to suppress the quasiparticle gap rendering any end state completely delocalized across the wire.³ In Figs.3 and 4 we present our predicted results for the tunnel conduc-

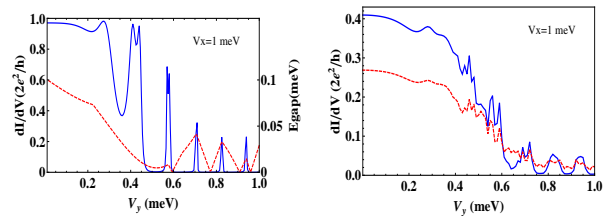


FIG. 4: (Left Panel) ZBCP as a function of V_y for a fixed $V_x = 1$ meV at zero temperature denoted by the blue solid line. ZBCP shows a plateau for small extent of V_y and is then suppressed by larger V_y . The red dashed line denotes the quasiparticle energy gap. The peaks appear after gap closure. (Right Panel) Blue solid and red dashed lines denote different temperature $T = 60$ and 120 mK, respectively. At finite temperature the ZBCP is suppressed. ($L = 4.5 \mu m$, spin-orbit coupling $\alpha = 0.2$ meVÅ, induced pairing potential $\Delta = 0.5$ meV)

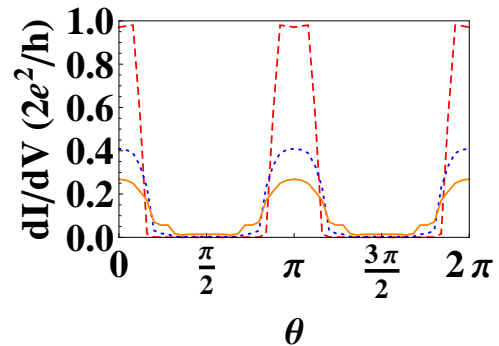


FIG. 5: ZBCP as a function of angle $\theta = \tan^{-1}(V_y/V_x)$ for a fixed $|V| = 1$ meV at $T = 0, 60, 120$ mK denoted by the red dashed, blue dotted and orange solid lines, respectively. ($L = 4.5 \mu m$, spin-orbit coupling $\alpha = 0.2$ meVÅ, induced pairing potential $\Delta = 0.5$ meV).

tance for different finite values of (V_x, V_y) . It is clear from Fig.3 that increasing V_y first suppresses the value of the ZBCP (at finite $T = 60$ mK), eventually making it disappear (as expected). For our chosen parameters for the system, the ZBCP essentially disappears for $V_y \sim \Delta \sim 0.5$ meV. In Fig.4 we plot the actual value of the differential conductance at the ZBCP as a function of V_y for $V_x = 1$ meV for $T = 60$ and 120 mK, and it is clear that ZBCP would disappear for $V_y \sim V_x$, particularly at higher temperatures. We therefore predict that the experimentally observed ZBCP signature in Ref.[1], for our estimates of the parameters of the experiment, should essentially completely disappear for the tilt angle $\theta \gtrsim 45^\circ$. An interesting notable (and experimentally verifiable) feature apparent in Fig.4 is that the ZBCP is quite immune to a finite V_y until V_y becomes reasonably large (> 0.4 meV for our chosen parameters) when it is suppressed reasonably quickly. The recent experimental study of the ZBCP¹, in fact, has studied the evolution

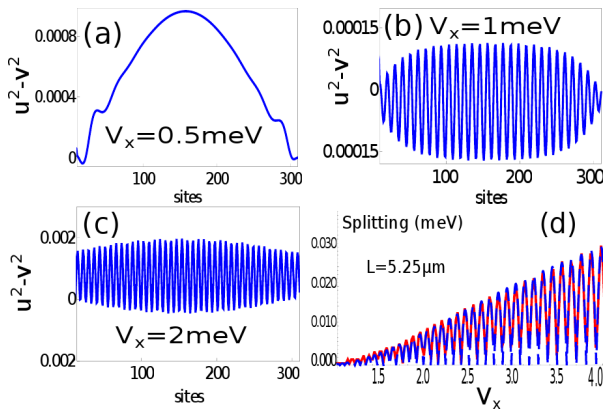


FIG. 6: Panels (a),(b) and (c) show the evolution of the charge density $u^2 - v^2$ of the split MFs generated by overlap for $L = 4.5 \mu\text{m}$ wire with different values of applied Zeeman-field V_x . Increasing V_x increases the overlap between MFs, which in turn leads to a finite charge $|u|^2 - |v|^2 \neq 0$ associated with the split Majorana fermion. Panel (d) shows the splitting of the Majorana fermion energy resulting from the same overlap as a function of Zeeman-field V_x . The red line is calculated result, while the blue dashed line is a fit to the analytically expected overlap as discussed in the text.

of the ZBCP as a function of transverse magnetic field V_y , by varying the angle $\theta = \tan^{-1}(V_y/V_x)$ in the plane of the wire, while holding the magnitude constant. In Fig.5 we present our numerical results for the ZBCP as a function of θ and we find oscillations of the ZBCP that are consistent with the experimental results in Ref.[1].

V. PROPOSED NEW EXPERIMENT

The splitting of the MFs shown in Fig.2 depends on the applied Zeeman field, V_x , and arises from overlap of the MF wave-functions localized at the two wire ends. The overlap of the MF wave-functions leads to Andreev states at non-zero energy which are no longer neutral i.e. $|u|^2 - |v|^2 \neq 0$ ²⁶ in contrast to the MF mode itself, which being a precise zero-energy mode must be precisely a neutral zero-charge quasiparticle. The total ground state charge density in the wire can in principle be calculated using the expression

$$\langle \rho(x) \rangle = \sum_{n: E_n < 0} \tanh \frac{E_n}{2k_B T} (|u_n(x)|^2 - |v_n(x)|^2), \quad (3)$$

where the Bogoliubov quasiparticle operators with energy E_n have the form $\Psi_n^\dagger = \int dx u_n(x) c^\dagger(x) + v_n(x) c(x)$. However, the charge density $\langle \rho(x) \rangle$ is influenced by the presence of disorder and one cannot in general separate the contribution of the background charge density from the charge density resulting from the splitting of MFs. The contribution of the split MFs to the charge density can be separated from the fixed background charge

density (which contains the contribution from impurity potentials) by controlling the occupancy of the split MF modes by coupling the ends of the superconducting system to an external normal fermionic lead. By changing the chemical potential of the normal fermionic lead, one changes the occupancy of the split MF modes, which leads to a change in the charge density in the case when the split MF modes are charged. The change in the charge density as a function of chemical potential of the normal fermion lead, which we refer to as "non-local compressibility" $\frac{\delta \langle \rho(x) \rangle}{\delta \mu_{lead}}$ separates out the effect of disorder from the charge of the split MFs. To calculate the non-local compressibility, we integrate out the normal fermionic lead creates a self-energy for the Bogoliubov states of the form

$$\Sigma_{lead}(\omega) = i\Gamma \tau_z \text{sgn}(\omega - \mu_{lead}), \quad (4)$$

where Γ is related to the transparency of the contact between the lead and the superconductor. This leads to an expression for the lead chemical potential μ_{lead} dependent charge density in the semiconductor

$$\langle \rho(x) \rangle (\mu_{lead}) = \sum_{n: E_n > 0} \tanh \frac{E_n - \mu_{lead}}{2k_B T} (|v_n(x)|^2 - |u_n(x)|^2). \quad (5)$$

The non-local compressibility defined as

$$\frac{\delta \langle \rho(x) \rangle}{\delta \mu_{lead}} = \frac{1}{T} \sum_{n: E_n > 0} \text{sech}^2 \frac{E_n - \mu_{lead}}{2k_B T} (|v_n(x)|^2 - |u_n(x)|^2), \quad (6)$$

can in principle²⁷ be measured-using single-electron-transistor (SET) spectroscopies in lock-in-mode^{28,29}. At low temperatures T , the compressibility singles out the split MF states near the chemical potential $E_n \sim \mu_{lead}$. When the value of μ_{lead} coincides with the energy E_n , there would be a peak in the non-local compressibility. The spatial profile of this peak is related to $|u|^2 - |v|^2$, which as shown in Fig.6 would show an oscillatory profile in space whose magnitude increases with the strength of the Zeeman field V_x . Here one has ignored the screening properties of the superconducting density of states. However, if only part of the nanowire is covered by the superconductor and the screening length of carriers in the nanowire is long compared to the oscillation wave-vector shown in Fig.6, the electrostatic screening effects of this charge density are not expected to be significant. Fig.6(d) shows the MF energy splitting resulting from the Zeeman splitting. This splitting (shown by the red curve) also oscillates as a function of the Zeeman splitting V_x . The splitting results from the overlap of the MF wave-functions¹⁸, which in the case of semiconductor nanowires has been shown to have the form³ $\psi(L/2) = \psi_0 e^{i(i\xi^{-1}(V_x) + k_F(V_x))L/2}$. The resulting MF overlap and splitting have the form splitting $e^{-L/\xi(V_x)}(a + bV_x) \cos(k_F(V_x)L + c + dV_x)$ where a, b, c, d are fitting parameters. As seen in Fig.6(d), we find the parameters (a, b, c, d) can be chosen to fit the V_x dependence over

a large range. This shows that the splitting of the low-energy eigenstates arising from the end of the nanowires shown in Fig.6 is consistent with resulting from the overlap of the localized end MFs.

The above discussion and the results presented in Fig.6 provide an exciting possibility for a scanning SET-based measurement and detection of the MF mode in semiconductor hybrid structures by measuring directly the charge associated with the split ZBCP modes in large Zeeman fields (where the end MFs overlap leading to MF-splitting), and then extrapolating this back to zero-splitting which should correspond to the neutral MF. This is by no means an easy experiment, but in principle, it is doable using existing SET techniques, and the spatially-resolved MF information coming out of such an experiment would be invaluable in understanding the details not only about the existence of the MF, but also about its wavefunction and its spatial location.

VI. DISCUSSION: DISORDER AND OTHER EFFECTS

The theoretical work and the numerical results presented in this work are based on a simple effective model which neglects many complications of the real system studied in the experiment. For example, although it is straightforward to include disorder in our model by adding a random one-particle potential in the tight-binding Hamiltonian, we have ignored providing results including effects of disorder because disorder effects have already been studied elsewhere in the literature,³⁰ and the details of the disorder operational in the experimental systems are not known. The main effect of disorder is to suppress the topological gap (and to eventually destroy it for disorder strength comparable to the gap size), and the specific experimental observations under consideration in the current work (namely, the suppression of ZBCP height, the Majorana splitting, the magnetic field effects, etc.) are unlikely to be qualitatively modified by disorder, particularly for the relatively clean wires studied in Ref.[1]. Our work also neglects any orbital coupling introduced by the magnetic field which could affect some of the experimental findings at very large fields where the magnetic length could be shorter than the wire width. Another limitation of the current theory is to approximate the tunneling measurement simply by a single tunneling barrier height U (and the finite wire length) without considering the actual details of the tunnel junction used in the experiments. This would necessitate a careful modeling of the tunnel contact which is well beyond the scope of the current minimal model. A full understanding of the experimental details must await a more quantitative realistic modeling of the actual semiconductor-superconductor hybrid structure used in the laboratory, which may, however, be challenging since many details (e.g. the nature of various interfaces) are unknown.

Two specific new results arising from our theoretical

work are partially in agreement with observations: the large suppression of the ZBCP height compared with the pristine theoretical quantization ($2e^2/h$) and the splitting of the ZBCP at large magnetic fields. Even for these two predictions, questions could be raised if alternate mechanisms are operational. The strong dependence of the actual ZBCP on the wire length and the tunnel barrier that we find in our results establishes that temperature by itself is insufficient to explain the quantitative height of the ZBCP, but neither the precise effective wire length nor the tunnel barrier height are known, again making a comparison between theory and experiment problematic at a quantitative level. False color images can easily be produced by adjusting various parameters making theory and experiment look alike, but this may not be particularly useful in view of the large number of unknowns in the problem. The Majorana splitting at high magnetic fields is inevitable due to the increasing magnitude of the dimensionless separation between the two end Majorana modes (as a ratio of the coherence length which increases monotonically with increasing field due to the suppression of the gap), and thus all experimental observations of the Majorana in real systems with finite wire lengths must eventually reflect this splitting. The Majorana splitting of the ZBCP should not behave as a simple linear function of the magnetic field distinguishing it clearly from any trivial Zeeman splitting. A clear prediction of the theory is that the splitting should oscillate in some manner, and such oscillations have not yet been seen experimentally. Whether the non-observation of the Majorana splitting oscillation is a genuine feature or is due to disorder and thermal broadening is unclear at this stage. Only further work can clarify this question.

VII. CONCLUSION

Before concluding, we point out that there are various resonance structures in our numerical results which arise from the sharpness of our confinement and transport models, which are completely non-universal and non-topological in nature. Such resonant structures in the current-voltage characteristics are well-known in 1D systems^{3,31} and arise from various resonances in the transmission and reflection coefficients. Presence of discrete impurities may lead to additional non-topological resonant structures. These resonant structures will shift around with gate voltage and magnetic field with the ZBCP being the only universal topologically robust feature in the data.

We mention that although the results presented in this work are restricted to the one-subband strict 1D limit (i.e. very large inter-subband gap energy) with no disorder, we have carried out some representative calculations for multisubband-occupied disordered wires finding qualitatively similar results, leading to our belief that our results and conclusions presented in this work continue to apply qualitatively in more realistic multisub-

band wires in the presence of finite disorder (provided a TS phase can be realized in the system). While any detailed quantitative comparison between experiment and theory must await more realistic modelling of the actual SM/SC systems utilized in Ref.[1], our current work decisively demonstrates that the suppression of the ZBCP well below the canonically quantized value, splitting of the ZBCP at high Zeeman fields, and the suppression of the ZBCP in the presence of a Zeeman field along the spin-orbit direction are all expected theoretical features of the SM/SC Majorana system proposed in Refs.[2–5] and observed in Ref.[1]. In addition, we propose a possible new experiment using the scanning SET spectroscopy, which, in principle, can provide information about the spatial location of the MF and its wavefunction by measuring the effective charge on the Andreev bound states associated with the splitting of the MFs in a finite wire at higher values of the Zeeman field.

Our work here is an extension and generalization of the standard theory for the Majorana mode^{2–5} to finite wire lengths at finite temperatures. This is important for the comparison with the experiment¹ at a qualitative level since this directly tells us the extent to which the standard zeroth order theory captures the essential features of the experiment. We do not introduce any new ingredient except to extend the standard theory to the experimental finite systems at finite temperatures so that an honest and direct assessment is possible about the key issue of whether the experiment of Ref.[1] really explores the theoretical predictions of Refs.2-5. Such a comparison with the extended standard theory is essential to establish future directions of research in this subject. We do find several surprises in our results of applying the standard theory to finite systems corresponding to finite length nanowires used in the experiments. For example, the ZBCP never reaches its expected quantized value in finite length wires even at very low temperatures because the details of the tunneling barrier now become an important variable. Another somewhat unexpected result, which should be checked in future experiments, is an oscillatory splitting of the MF as a function of the effective Zeeman splitting at high values of the magnetic field where the topological gap is sufficiently suppressed so that the coherence length is larger than the wire length.

We conclude by stating that we have established in this work that the two puzzling features of the likely experimental observation of the Majorana modes in 1D InSb nanowire¹ following earlier theoretical proposals^{2–5} can be explained by including finite wire length, finite temperature, and finite tunneling barrier effects in the theory. We have also made specific predictions on how the zero-bias-conductance peak will be suppressed in the presence of a finite magnetic field in the transverse direction and how the Majorana-induced zero-bias-

conductance-peak will split at high Zeeman splitting in a finite wire due to the overlap between the Majorana modes at the two ends of the wire. Our work does not prove that the experiment reported in Ref.[1] is indeed the experimental discovery of the long-awaited Majorana fermion, particularly since unknown effects could, in principle, conspire to give a weak zero bias peak which follows for unknown reasons the phenomenology observed in the experiment and theoretically modeled in the current work. What our work does provide is compelling support for the claim that the observation of Ref.[1] is indeed consistent with the theoretically predicted existence of the MF in semiconductor hybrid structures, and the apparent anomalies in the data of Ref.[1] (suppressed ZBCP, high-field splitting of the ZBCP, etc.) are all completely in accord with the zeroth order theory. The absolute confirmation of the solid state MF discovery must await a direct demonstration of the non-Abelian nature of these quasiparticles through an interferometry measurement which however is unlikely to be either easy or quick. Meanwhile, further observations of ZBCP in other nanowires by different groups and various consistency checks between theory and experiment, as carried out in the current work, would go a long way in establishing that perhaps the elusive Majorana has finally shown up in a most unusual place, in a semiconductor placed on a superconductor in the presence of Zeeman spin splitting.

This work is supported by Microsoft Q and JQI-NSF-PFC. J. S. acknowledges support from the Harvard Quantum Optics Center.

Note added: After the posting of our work, the results of Ref.[1] appeared on line in its published form³². All our results, discussion, and conclusion with respect to Ref.[1] apply equally well to the published results in Ref.[32]. Thus, the case in favor of the likely experimental observation^{1,32} of the possible signatures for the existence of the proposed^{2–5} Majorana modes in SM/SC hybrid structures is further enhanced by our theoretical results. We point out, however, that at best the observations of Refs.[1,32] establish only the necessary conditions for the existence of the long-sought emergent Majorana modes in solid state systems. Much more work would be needed, including the observation of similar effects in other semiconductor nanowires with strong spin-orbit coupling (e.g. InAs) and the experimental demonstration of the sufficient conditions for the existence of the Majorana modes involving the observation of the fractional Josephson effect^{4,8,33} and/or the non-Abelian braiding³⁴, before one can compellingly claim to have discovered the elusive Majorana quasiparticles in solid state systems.

¹ V. Mourik, K. Zuo, S. M. Frolov, S. R. Plissard, E. P. A. M. Bakkers, and L. P. Kouwenhoven Science, 1222360

(2012).

- ² J. D. Sau, R. M. Lutchyn, S. Tewari, S. Das Sarma, Phys. Rev. Lett. **104**, 040502 (2010).
- ³ J. D. Sau, S. Tewari, R. Lutchyn, T. Stanescu and S. Das Sarma, Phys. Rev. B **82**, 214509 (2010).
- ⁴ R. M. Lutchyn, Jay D. Sau, S. Das Sarma, Phys. Rev. Lett. **105**, 077001 (2010) .
- ⁵ Y. Oreg, G. Refael, F. V. Oppen, Phys. Rev. Lett. **105**, 177002 (2010).
- ⁶ E. Reich, Nature **483**, 132 (2012); F. Wilczek, Nature **486**, 195 (2012); P. Brouwer, Science **25**, 989 (2012); R. Service, Science **332**, 193 (2012); R. Wilson, Physics Today **65**, 14 (2012)
- ⁷ R. M. Lutchyn, T. Stanescu, S. Das Sarma, Phys.Rev.Lett. **106**, 127001 (2011).
- ⁸ A. Y. Kitaev, Physics-Uspekhi **44**, 131 (2001).
- ⁹ K. Sengupta, I. Zutic, H. Kwon, V. M. Yakovenko, and S. Das Sarma, Phys. Rev. B **63**, 144531 (2001).
- ¹⁰ T. Stanescu, R. M. Lutchyn, S. Das Sarma, Phys. Rev. B **84**, 144522 (2011)
- ¹¹ K. Flensberg, Phys. Rev. B. **82**, 180516(R) (2010)
- ¹² Jay D. Sau, Sumanta Tewari, and S. Das Sarma, Phys. Rev. B **85**, 064512 (2012)
- ¹³ K. T. Law, Patrick A. Lee, and T. K. Ng, Phys. Rev. Lett. **103**, 237001 (2009).
- ¹⁴ E. Prada, P. San-Jose, R. Aguado, arXiv:1203.4488 (2012); J. Lim, L. Serra, R. Lopez, R. Aguado, arXiv:1202.5057 (2012)
- ¹⁵ M. Wimmer, A.R. Akhmerov, J.P. Dahlhaus, C.W.J. Beenakker, New J. Phys. **13**, 053016 (2011).
- ¹⁶ S. Nadj-Perge, V. S. Pribiag, J. W. G. van den Berg, K. Zuo, S. R. Plissard, E. P. A. M. Bakkers, S. M. Frolov, L. P. Kouwenhoven. e-print arXiv:1201.3707
- ¹⁷ C. J. Bolech, E. Demler, Phys. Rev. Lett. **98**, 237002 (2007).
- ¹⁸ M. Cheng, R. M. Lutchyn, V. Galitski, S. Das Sarma, Phys. Rev. Lett. **103**, 107001 (2009).
- ¹⁹ H. A. Nilsson, P. Samuelsson, P. Caroff, and H. Q. Xu Nano Letters **12**, 228 (2012).
- ²⁰ L. P. Rokhinson, private communication .
- ²¹ C. M. Marcus, private communication.
- ²² Y. J. Doh et al., Science **309**, 272 (2005).
- ²³ G. E. Blonder, M. Tinkham, and T. M. Klapwijk, Phys. Rev. B **25**, 4515 (1982).
- ²⁴ Meng Cheng, Roman M. Lutchyn, Victor Galitski, S. Das Sarma, Phys. Rev. B **82**, 094504 (2010).
- ²⁵ P. Ghosh, J. D. Sau, S. Tewari, S. Das Sarma, Phys. Rev. B, **82**, 184525 (2010).
- ²⁶ J. D. Sau, S. Tewari, S. Das Sarma, Phys. Rev. B **84**, 085109 (2011)
- ²⁷ A. Yacoby, private communication.
- ²⁸ M. J. Yoo et al., Science **276**, 579 (1997).
- ²⁹ S. Ilani, A. Yacoby, D. Mahalu, H. Shtrikman, Science **292**, 1354 (2001); V. Venkatachalam, A. Yacoby, L. Pfeiffer, K. West, Nature **469**, 185 (2011)
- ³⁰ A. C. Potter, P. A. Lee, Phys. Rev. B **83**, 184520 (2011); T. D. Stanescu, R. M. Lutchyn, S. Das Sarma, Phys. Rev. B **84**, 144522 (2011); R. M. Lutchyn, T. D. Stanescu, S. Das Sarma, Phys.Rev.Lett. **106**, 127001 (2011); R. M. Lutchyn, T. D. Stanescu, S. Das Sarma, Phys. Rev. B **85**, 140513(R) (2012); P. W. Brouwer, M. Duckheim, A. Romito, F. von Oppen , Phys. Rev. Lett. **107**, 196804 (2011); P. W. Brouwer, M. Duckheim, A. Romito, F. von Oppen ,Phys. Rev. B **84**, 144526 (2011); J. D. Sau, S. Tewari, S. Das Sarma, Phys. Rev. B **85**, 064512 (2012).
- ³¹ Song He and S. Das Sarma, Phys. Rev. B **48**, 4629 (1993).
- ³² V. Mourik, et al., arXiv:1204.2792; Science Express April 12, on line 1222360 (2012).
- ³³ H.J. Kwon et al., Eur. Phys. J. B **37**, 349 (2004)
- ³⁴ F. Hassler, A. R. Akhmerov, C.-Y. Hou, C. W. J. Beenakker, New J. Phys. **12**, 125002 (2010); J. D. Sau, S. Tewari, S. Das Sarma, Phys. Rev. A **82**, 052322 (2010); J. Alicea, Y. Oreg, G. Refael, F. von Oppen, M. P. A. Fisher, Nature Physics **7**, 412 (2011); J. D. Sau, D. J. Clarke, S. Tewari Phys. Rev. B **84**, 094505 (2011); B. I. Halperin, Y. Oreg, A. Stern, G. Refael, J. Alicea, and F. von Oppen, Phys. Rev. B **85**, 144501 (2012); B. van Heck, A.R. Akhmerov, F. Hassler, M.Burrello, C.W.J. Beenakker, New J. Phys. **14** 035019 (2012).